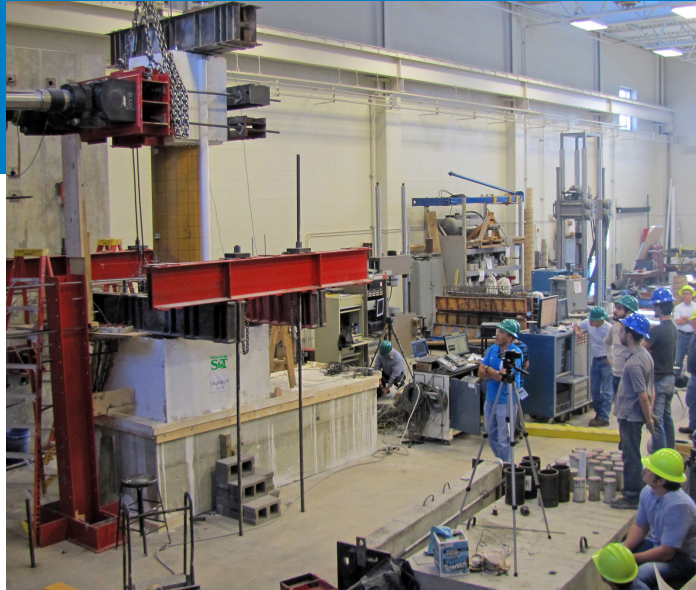


An ACI Technical Publication

SYMPOSIUM VOLUME



Structural Performance of Concrete  
Columns Incorporating Advanced  
Materials and Structural Systems

SP-341

Editor:  
Mohamed A. ElGawady



American Concrete Institute  
*Always advancing*



# Structural Performance of Concrete Columns Incorporating Advanced Materials and Structural Systems

Sponsored by  
ACI Committees 441 – Reinforced Concrete  
Columns and 341A – Earthquake-Resistant  
Concrete Bridge Columns

The Concrete Convention and Exposition  
October 14-18, 2018  
Las Vegas, NV

Editor:  
Mohamed A. ElGawady



American Concrete Institute  
*Always advancing*

SP-341

First printing, June 2020

Discussion is welcomed for all materials published in this issue and will appear ten months from this journal's date if the discussion is received within four months of the paper's print publication. Discussion of material received after specified dates will be considered individually for publication or private response. ACI Standards published in ACI Journals for public comment have discussion due dates printed with the Standard.

The Institute is not responsible for the statements or opinions expressed in its publications. Institute publications are not able to, nor intended to, supplant individual training, responsibility, or judgment of the user, or the supplier, of the information presented.

The papers in this volume have been reviewed under Institute publication procedures by individuals expert in the subject areas of the papers.

Copyright © 2020  
AMERICAN CONCRETE INSTITUTE  
38800 Country Club Dr.  
Farmington Hills, Michigan 48331

All rights reserved, including rights of reproduction and use in any form or by any means, including the making of copies by any photo process, or by any electronic or mechanical device, printed or written or oral, or recording for sound or visual reproduction or for use in any knowledge or retrieval system or device, unless permission in writing is obtained from the copyright proprietors.

Printed in the United States of America

Editorial production: Ryan M. Jay

ISBN-13: 978-1-64195-105-0

## **PREFACE**

Columns are crucial structural elements in buildings and bridges. This Special Publication of the American Concrete Institute Committees 441 (Reinforced Concrete Columns) and 341A (Earthquake-Resistant Concrete Bridge Columns) presents the state-of-the-art on the structural performance of innovative bridge columns. The performance of columns incorporating high-performance materials such as ultra-high-performance concrete (UHPC), engineered cementitious composite (ECC), high-strength concrete, high-strength steel, and shape memory alloys is presented in this document. These materials are used in combination with conventional or advanced construction systems, such as using grouted rebar couplers, multi-hinge, and cross spirals. Such a combination improves the resiliency of reinforced concrete columns against natural and man-made disasters such as earthquakes and blast.



## TABLE OF CONTENTS

### **SP-341-1:**

Behavior of High-Strength Concrete and Normal-Strength Concrete Columns  
under Blast Loading ..... 1-26  
Authors: Amer Hammoud and Hassan Aoude

### **SP-341-2:**

Combined use of UHPC and High-Performance Steel to Improve the  
Blast Performance of Columns with Square Cross-section..... 27-47  
Authors: Sarah De Carufel and Hassan Aoude

### **SP-341-3:**

Parameters Affecting the Axial Load Response of Ultra High Performance  
Concrete (UHPC) Columns.....48-70  
Authors: Hyun-Oh Shin, Hassan Aoude and Denis Mitchell

### **SP-341-4:**

Comparative Structural Response of UHPC and Normal Strength Concrete  
Columns under Combined Axial and Lateral Cyclic Loading..... 71-96  
Authors: Mahmoud Aboukifa, Mohamed A. Moustafa and Ahmad Itani

### **SP-341-5:**

Cyclic Behavior of a Reinforced Concrete Column with Unstressed Seven-Wire  
Steel Strands as Longitudinal Reinforcement ..... 97-104  
Authors: Yu-Chen Ou, Samuel Y.L.Yin, Yi-Qing Liu, and Jui-Chen Wang

### **SP-341-6:**

Analysis and Design of NiTi Superelastic SMA-Reinforced ECC Bridge Columns.... 105-130  
Authors: Mostafa Tazarv and M. Saiid Saiidi

### **SP-341-7:**

Seismic Fragility Assessment of Shape Memory Alloy Reinforced Concrete  
Bridge Piers under Long Duration and Near-Fault Ground Motions ..... 131-159  
Authors: Maher AL-Hawarneh, AHM Muntasir Billah, and M. Shahria Alam

### **SP-341-8:**

Experimental Investigation on Mechanical Properties of Titanium Alloy Bars:  
Comparison with High-Strength Steel..... 160-187  
Authors: Ruchin Khadka, Mustafa Mashal, and Jared Cantrell

**SP-341-9:**

Seismic Behavior of Bridge Precast Columns with Grouted Rebar Couplers..... 188-201  
Authors: Arya Ebrahimpour and Barbara Earles

**SP-341-10:**

Using Multi-“Hinge” Hierarchical Activation to Improve Structural Robustness..... 202-225  
Authors: Royce Liu and Alessandro Palermo

**SP-341-11:**

Using Cross Spirals in Confining High Strength Concrete Columns for  
More Seismic Resiliency: A Review ..... 226-239  
Authors: Ahmed Ibrahim, Sabreena Nasrin, and Riyadh Hindi

## **Behavior of High-Strength Concrete and Normal-Strength Concrete Columns under Blast Loading**

Amer Hammoud and Hassan Aoude

**Synopsis:** This paper presents the results from tests examining the performance of high-strength concrete (HSC) and normal-strength concrete (NSC) columns subjected to blast loading. As part of the study six columns built with varying concrete strengths were tested under simulated blast loads using a shock-tube. In addition to the effect of concrete strength, the effects of longitudinal steel ratio and transverse steel detailing were also investigated. The experimental results demonstrate that the HSC and NSC columns showed similar blast performance in terms of overall displacement response, blast capacity, damage and failure mode. However, when considering the results at equivalent blasts, doubling the concrete strength from 40 MPa to 80 MPa (6 to 12 ksi) resulted in 10%-20% reductions in maximum displacements. On the other hand, increasing the longitudinal steel ratio from  $\rho = 1.7\%$  to 3.4% was found to increase blast capacity, while also reducing maximum displacements by 40-50%. The results also show that decreasing the tie spacing (from  $d/2$  to  $d/4$ , where  $d$  is the section depth) improved blast performance by reducing peak displacements by 20-40% at equivalent blasts. The use of seismic ties also prevented bar buckling and reduced the extent of damage at failure. As part of the analytical study the response of the HSC columns was predicted using single-degree-of-freedom (SDOF) analysis. The resistance functions were developed using dynamic material properties, sectional analysis and a lumped inelasticity approach. The SDOF procedure was able to predict the blast response of HSC columns with reasonable accuracy, with an average error of 14%. A numerical parametric study examining the effects of concrete strength, steel ratio and tie spacing in larger-scale columns with 350 mm x 350 mm (14 in. x 14 in.) section was also conducted. The results of the numerical study confirm the conclusions from the experiments but indicate the need for further blast research on the effect of transverse steel detailing in larger-scale HSC columns.

**Keywords:** High-strength concrete, Columns, Blast, Shock Tube.

**Amer Hammoud** received his Master's (MAsc) degree from the Department of Civil Engineering at the University of Ottawa. He is currently a bridge engineer at Parsons in Ottawa, Canada.

ACI member **Hassan Aoude** is an Associate Professor in the Department of Civil Engineering at the University of Ottawa. He received his PhD from McGill University in Montreal, QC, Canada. His research interests include the blast behavior of high-performance and fiber-reinforced concretes.

## INTRODUCTION

The use of high-strength concrete (HSC) in structures has gradually increased over the past few decades. The American Concrete Institute (ACI) defines HSC as concrete that has a compressive strength which exceeds 55 MPa (8 ksi), however concretes with strengths of 80-100 MPa (12-15 ksi) are now regularly used in practice <sup>1</sup>. One of the established applications of HSC is in the lower storey columns of high-rise buildings, where its use can allow for reduced cross-section sizes and more efficient use of floor space <sup>2</sup>. As noted in ACI 363R-10: “*the largest application of HSC has been in the columns of high-rise buildings*” and “*all of the tallest buildings constructed in the past 10 years have some structural contribution from HSC in vertical column elements*” <sup>1</sup>.

Over the years, extensive studies have examined the behavior of HSC columns under pure axial compression and simulated earthquake loading. A comprehensive review of this research is summarized in ACI 441R-96: Report on High-strength Concrete Columns <sup>2</sup>. As a result of this important research, design requirements for the structural use of high-strength concrete in columns are now well established in several codes worldwide <sup>3</sup>. Comparatively very limited research exists on the blast performance of such columns. Given the critical role of ground-story columns in the overall blast resistance and stability of multi-story buildings <sup>4</sup>, there exist an important need for research data that can allow for better understanding of the blast behavior of HSC columns.

Accordingly, this paper examines the effect of increased concrete strength on the blast behavior of a series of columns tested under simulated blasts using a shock-tube. In addition to the effect of concrete strength, the effects of longitudinal steel ratio and seismic detailing are also investigated. As part of the analytical study the blast behavior of the test columns is predicted using dynamic inelastic single-degree of freedom (SDOF) analysis.

## REVIEW OF PREVIOUS BLAST RESEARCH ON RC COLUMNS

Important research has investigated the behavior of reinforced concrete columns under extreme dynamic loading, including impact and blast. The following sections provide a brief review of this research.

### Previous Impact Studies on Reinforced Concrete Columns

The impact behavior of reinforced columns has been investigated by a number of early researchers, including Reinschmidt et al. <sup>5</sup> and others. Louw et al. <sup>6</sup> conducted a more recent study on the impact response of reinforced concrete columns. A total of 28 cantilever columns having dimensions of 4 m × 300 mm × 300 mm (13 ft × 12 in. × 12 in.) were tested under drop-weight impact loads, with an additional 8 specimens tested under quasi-static conditions. Varying strain-rates were obtained by dropping a striker with varying masses (650-1450 kg [1430-3200 lb]) from 2.7 m (8.9 ft), resulting in impact velocities of 6.4-7.1 m/s (21-23 ft/s). The columns were subdivided into 8 groups based on the percentage of steel, concrete strength ( $f'_c = 19-37$  MPa [2.8-5.4 ksi]) and amount of axial load. The main conclusion of this study was that concrete strength and shear reinforcement had a greater influence on the shear resistance of the columns, while flexural strength was governed by the longitudinal reinforcement ratio. For shear-critical columns, doubling the concrete strength was found to increase the impact strength by 33%, compared to an increase of 17% under static conditions.

Remennikov and Kaewunruen <sup>7</sup> conducted another series of impact tests on five quarter-scale reinforced concrete columns ( $f'_c = 32$  MPa [4.6 ksi]) having dimensions of 1 m × 100 mm × 100 mm (40 in. × 4 in. × 4 in.) using a drop hammer test rig. The main parameters investigated were the drop-height (1.2-1.9 m [47-75 in.]) of the 160 kg (352 kg [776 lb.]) mass, and the column shear-bending capacity ratios (0.63-0.93). An additional 2 columns were tested statically. Since the shear/bending capacity ratios were less than 1, all impact-tested columns failed in shear, with diagonal cracks developing in a more severe manner when compared to static conditions. While the study found the dynamic reaction force can be enhanced by a factor of up to 2.0 under impact, the authors noted that flexural behavior under impact can only be developed if the shear capacity significantly exceeds bending resistance due to amplification of the reaction force under dynamic loading. The study further noted that columns with poorly confined concrete require an enhancement to their ductility to adequately resist impact loading.

Research on the impact response of HSC columns is scarce, however Huynh et al. <sup>8</sup> investigated the impact response of a series of sixteen 2 m × 250 mm × 250 mm (80 in. × 9.8 in. × 9.8 in.) high-strength concrete and reactive powder concrete (RPC) beams-columns ( $f'_c = 100-160$  MPa [15-23 ksi]) under low and medium-velocity impact loading. The effects of axial force, load eccentricity, and RPC as a replacement for HSC (in the cover/shell

region or the entire section) were investigated. The results showed that both axial load and load eccentricity had important effects on impact resistance and failure mode, while the use fiber-reinforced RPC was found to improve the impact performance of the columns when compared to HSC. Under static testing the HSC columns failed in flexure, whereas they experienced flexure-shear or shear failures under impact, with the authors noting that the change in failure mode was more noticeable for the HSC columns when compared to the RPC columns.

### **Previous blast studies on reinforced concrete columns**

Given the critical role of columns in the blast performance of buildings, a significant number of studies have focused on studying the blast behavior of reinforced concrete columns, both numerically and experimentally. Saatcioglu et al. <sup>9</sup> numerically studied the effect of seismic design on the blast response of RC frames using dynamic inelastic analysis. The authors concluded that seismic detailing improved the overall blast performance and ductility of the buildings, while noting that such detailing can reduce the potential of progressive collapse. Similar conclusions were reported by Hayes et al. <sup>10</sup>, where strengthening of perimeter column elements using modern seismic detailing requirements was found to reduce blast damage and prevent progressive collapse. Similarly, Bao and Li <sup>11</sup> used finite element modeling to examine the effects of transverse reinforcement spacing on the blast response of columns and noted that the use of seismic detailing improved control of deflections and increased residual capacity. Similar results have been reported by Kyei and Braimah <sup>12</sup> and others.

Experimental research on the blast behavior of conventional reinforced concrete columns has primarily focused on bridge type elements subjected to near-field or close-in blasts. Fujikura and Bruneau <sup>13</sup> conducted an important series of field tests on quarter-scale seismically-detailed bridge columns as well as non-ductile columns retrofitted with steel-jacketing. The NSC columns ( $f'_c = 42$  MPa [6 ksi]) had 300 mm (12 in.) circular cross-sections and were tested under close-in blasts, without axial loads. Converse to the above cited numerical research, the study found that the seismically-detailed and retrofitted columns did not show ductile response, and suffered brittle direct shear failures under blast loading. In a further series of companion tests, improved performance was obtained in concrete-filled circular steel tube (CFST) bridge piers designed using a multi-hazard concept <sup>14</sup>.

Williamson et al. <sup>15</sup> conducted another important series of tests on ten half-scale NSC ( $f'_c = 28$  MPa [4 ksi]) bridge columns, also under close-in blast loads. A large set of parameters were investigated, including the effect of standoff distance, column depth ratio, transverse steel detailing and splice location. Increasing the transverse steel ratio was found to improve the blast behavior of the columns, with the best performance obtained when using “blast” and “seismic” detailing when compared to “typical” design detailing. On the other hand, the failure mode under intense close-in blasts was also observed to be direct shear at the base.

Experimental studies on the behavior of RC columns subjected to far-field blasts are limited. Lloyd <sup>16</sup> studied the blast response of a series of normal-strength concrete columns ( $f'_c = 46$ -58 MPa [6.7-8.4 ksi]) having dimensions of 2.4 m  $\times$  0.1 m  $\times$  0.15 m (95 in.  $\times$  4 in.  $\times$  6 in.) and reinforced with varying steel ratios under simulated blast loads using a shock-tube. The study reported that the use of increased longitudinal steel ratio improved the displacement response of the columns, however the use of seismic vs conventional detailing was found to be insignificant. Conversely, Burrell et al. <sup>17</sup> reported that seismic detailing in self-consolidating concrete (SCC) columns ( $f'_c = 50$  MPa [7.3 ksi]) with larger 0.15m  $\times$  0.15m (6 in.  $\times$  6 in.) cross-sections reduced displacements, prevented bar buckling and increased damage tolerance.

To the knowledge of the authors there exists no published studies on the blast behavior of conventional HSC columns, whether under close-in or far-field explosions. Nonetheless, a few studies in the literature have focused on more advanced UHPC (ultra-high performance concrete). For example, Astarlioglu and Krauthammer <sup>18</sup> numerically studied the blast response of NSC and UHPC columns using SDOF analysis and noted that the use of UHPC improved control of displacements and significantly increased the impulse required to cause failure. Similar conclusions related to the benefits of using UHPC in columns have been reported in the experimental studies conducted by Xu et al. <sup>19</sup> (near-field blasts) and Aoude et al. <sup>20</sup> (far-field, simulated blasts).

In addition to new structures, several researchers have also studied the potential of various retrofits to increase the blast resistance of existing RC columns. Among them, an important number of studies have focused on the effectiveness of using fiber-reinforced plastics (FRP) to improve the blast behavior of columns (for a review, see Crawford <sup>21</sup>). Other retrofit techniques considered in the literature include the use of steel-jackets <sup>13</sup> and steel-reinforced polymer (SRP) wraps <sup>22</sup>.

## **RESEARCH SIGNIFICANCE**

The previous sections provided an overview of published studies which have focused on the impact and blast behavior of reinforced concrete columns. While important tests and conclusions have been reported in the literature, the blast behavior of high-strength concrete columns has not been specifically studied by other researchers. Previous research is also conflicting about the effectiveness of seismic detailing to improve the blast

behavior of reinforced concrete columns. Experimental studies on the blast behavior of columns subjected to far-field blasts also remain relatively limited. Accordingly, this paper aims to fill this gap in research and increase the understanding of the effect of increased concrete strength on the blast behavior of columns, with a particular focus on columns subjected to far-field type blasts. In addition to examining the effect of concrete strength, the tests provide insights into the effects of seismic detailing and longitudinal steel ratio on the blast behavior of the HSC columns. To further examine the influence of increased concrete strength, the response of the HSC columns is compared to ultra-high strength UHPC columns previously tested by the authors.

## EXPERIMENTAL INVESTIGATION

### Description of specimens

A total of six columns were built and tested in this research program. The tests included two columns cast with normal-strength concrete (NSC) and four columns built with high-strength concrete (HSC). The HSC series included specimens with and without seismic detailing, while the effect of longitudinal steel ratio was investigated in both concrete series. **Table 1** and **Fig. 1** summarize the design details of the test specimens.

As shown in **Fig. 1**, all columns had a total height of 2.44 m (8 ft) and cross-sectional dimensions of 152 mm × 152 mm (6 in. × 6 in.). Longitudinal reinforcement consisted of 4 – 10M, 4 – No.4, or 4 – 15M bars (bar diameters = 9.5, 11.3, 16 mm [0.38, 0.44, 0.63 in.], with bar areas = 71, 100, 200 mm<sup>2</sup> [0.11, 0.16, 0.31 in<sup>2</sup>]), resulting in longitudinal steel ratios of 1.7%, 2.2% and 3.4%. Transverse reinforcement in all “non-seismic” columns consisted of 6.3 mm (0.25 in.) diameter ties made of non-deformed steel wire, spaced at  $s = 75$  mm (3 in.), conforming to the requirements of *moderately ductile* columns in the CSA A23.3 Standard (ductility-related factor,  $R_d = 2.5$ )<sup>23</sup>. This spacing was reduced to 38 mm (1.5 in.) in one “seismic” HSC column, following the requirements of *ductile* columns in the same standard ( $R_d = 4$ ). In all cases, the tie spacing was kept constant over the column height.

Specimen nomenclature in **Table 1** reflects the three variables in the experimental program, namely: the concrete type (HSC vs. NSC), longitudinal bar size (10M, No.4 or 15M bars), and transverse steel detailing level (with “S” indicating use of seismic ties). For example, column NSC-10M was built with normal-strength concrete, 4-10M bars and non-seismic ties spaced at 75 mm (3 in.), while HSC-10M-S represents the companion column built with HSC and seismic ties spaced at 38 mm (1.5 in.)

### Material properties

**Table 2** lists the properties of the normal-strength and high-strength concrete mixes used in this study. The NSC mix had a specified strength of 35 MPa (5.1 ksi), with a maximum aggregate size of 19 mm (0.75 in.) and contained no admixtures. The high-strength concrete mix had a target strength of 80 MPa (11.6 ksi), and its constituents included Portland cement, slag, silica fume, sand, coarse aggregate (with a maximum size of 9.5 mm [3/8 in.]) and liquid admixtures (a water reducer and set retarder). In all cases the concrete was mixed using a 0.225 m<sup>3</sup> (8 ft<sup>3</sup>) capacity forced-action pan mixer at the University of Ottawa. The average properties of the concrete in each column in terms of compressive strength were obtained by testing three 100 mm × 200 mm (4 in. × 8 in.) cylinders on the day of testing in accordance with the ASTM C39 standard (see **Table 1**). The properties of the steel reinforcement were obtained from tension tests on a minimum of 3 samples for each bar type in accordance with the ASTM 370 standard<sup>24</sup> (see **Table 3**). Based on these tests, the average yield strengths of the 10M, No.4, 15M bars and 6 mm wire were determined to be 474, 464, 449 and 542 MPa (69, 67, 65 and 79 ksi). **Fig. 2** shows typical stress-strain curves for the NSC, HSC and steel reinforcement.

### University of Ottawa Shock Tube

The University of Ottawa Blast Research Laboratory is equipped with a shock-tube that can simulate the shockwaves generated by the hemispherical free air surface burst of high explosives<sup>25</sup>. As shown in **Fig. 3a**, the shock tube consists of four main components, including: (1) a variable length driver section which generates the shockwave energy using compressed air, (2) a spool section which controls the firing of the shockwave using a differential pressure diaphragm, (3) and an expansion section which ends with (4) a 2 m × 2 m (80 in. × 80 in.) rigid end test frame. For non-planar elements such as columns, a load transfer device (LTD) is used to collect and transfer the pressure at the end-frame opening onto the specimens. Varying shockwave parameters (pressure, duration and impulse) can be obtained by adjusting the shock-tube driver length and driver pressure.

### Test setup and procedure

**Fig. 3b** shows a typical column prior to testing. All columns were tested under combined axial and blast loads. For all tests the axial load at the start of the tests was 294 kN (66 kip), equivalent to ~ 30% of the pure axial load capacity of the control normal-strength concrete specimens. In this study the LTD consisted of a light gauge steel metal sheet connected to a series of steel beams which resulted in the transfer of the blast pressure as a uniformly

distributed load along the tension face of the columns. The clear span of the columns between supports was 1980 mm (6.5 ft), with the columns connected to the shock-tube frame using partially-fixed supports. Complete displacement-time histories were recorded using two linear variable differential transducers (LVDT) placed at mid-height and at 1/3<sup>rd</sup> distance along the clear span as shown in **Fig. 3b**. Pressure sensors near the load transfer device were used to record complete reflected pressure time histories for each test. A high speed camera also recorded the response of the columns response at a frame rate of 500 frames per second.

Each column was tested with gradually increasing blast pressures to test the specimens under elastic, yield and ultimate conditions. Sample shockwaves corresponding to Blasts 1 to 4 are shown in **Fig. 4a**. In this study, the driver length was kept constant at 2743 mm (9 ft) while the driver pressures varied between 17 psi (117 kPa), 35 psi (240 kPa), 80 psi (550 kPa) and 100 psi (690 kPa) for Blasts 1 to 4, respectively. The resulting average reflected pressure ( $P_r$ ), positive phase duration ( $t_d$ ), and reflected impulse ( $I_r$ ) for these blasts are summarized in **Table 4**.

## EXPERIMENTAL RESULTS

### Summary of results

**Table 5** summarizes the detailed experimental results for the columns in terms of measured shockwave parameters ( $P_r$ ,  $t_d$ , and  $I_r$ ) and column responses (maximum midspan displacements, residual midspan displacements and support rotations:  $d_{max}$ ,  $d_{res}$  and  $\theta_{max}$ ). **Fig. 4b** shows typical blast and response time histories for one column. **Fig. 5-7** show photos of the columns illustrating damage, and **Fig. 8-11** compare the column displacement responses at selected blasts. It is noted that displacements  $d_{max}$  and  $d_{res}$  (and the results in the figures) represent “net” values (i.e. displacements were zeroed before each test). For reference,  $d_{max}^c$  and  $d_{res}^c$  represent the cumulative displacements, which include the permanent deflections from previous shots (see **Table 5**). **Table 5** also compares the net rotations with the response limits in the CSA S850 blast standard<sup>36</sup>. These response limits (B1-B4) correspond to specific values of support rotation ( $\theta_{max}$ ) or ductility ratio ( $\mu_{max}$ ). In this study, response limits B1, B2, B3 and B4 were defined using  $\mu_{max} = 1$ ,  $\theta_{max} = 4^\circ$ ,  $\theta_{max} = 6^\circ$  and  $\theta_{max} = 10^\circ$ , respectively. These limits in turn define component damage levels: “Blowout” (greater than B4), “Hazardous failure” (between B4 and B3); “Heavy” (between B3 and B2); “Moderate” (between B2 and B1) and “Superficial” (less than B1). In this study, Blast 1 tested the columns under elastic conditions ( $\mu_{max} \leq 1$ ) and aimed at causing “superficial” damage, while Blast 2 was intended to bring the longitudinal steel in most columns near yielding and cause “moderate” damage ( $\theta_{max} \leq 4^\circ$ ). Blasts 3 and 4 were intended to cause “heavy” ( $4^\circ < \theta_{max} \leq 6^\circ$ ) and “hazardous” damage ( $6^\circ < \theta_{max} \leq 10^\circ$ ), respectively.

### Effect of parameters on midspan displacements

In this section the results from Blasts 1-4 are compared to investigate the effects of the test parameters on maximum and residual displacements, support rotations, blast capacity and failure mode.

Effect of concrete strength — The effect of concrete strength can be examined by comparing the response of the following two sets of specimens which were built with high-strength concrete and normal-strength concrete, respectively: 1) HSC-#4 vs. NSC-#4 and 2) HSC-15M vs. NSC-15M. It is noted that all four columns had non-seismic ties, with 4-No.4 and 4-15M bars used in Sets 1 and 2, respectively. Comparative displacement results for these columns are shown in **Fig. 8**.

In the No.4 set the two companion columns recorded similar displacements at Blasts 1 and 2 (17 and 35 psi), with support rotations of  $\theta_{max} \approx 0.5^\circ$  and  $\theta_{max} \approx 1.2^\circ$ . Damage was limited to hairline cracks at Blast 1 and further crack opening at Blast 2, which can indeed be qualified as “superficial” and “moderate”. The low residual displacements also confirm that Blast 1 kept the columns in the elastic range, while the permanent deformations at Blast 2 confirm that this shot brought the columns to inelastic conditions. Both columns sustained large displacements and significant damage at Blast 3 (80 psi), however reductions of 6% and 14% in maximum and residual displacements were recorded for the HSC column when compared to its NSC companion (**Fig. 8a**). The support rotations for these columns reached  $\theta_{max} = 4.8^\circ$  and  $5^\circ$ , with signs of concrete crushing and the formation of plastic hinges at midspan and at the column ends (**Figs. 5a & 5e**), which can indeed be qualified as “heavy” damage. Only column HSC-#4 was tested under a fourth shot (Blast 4 – 100 psi), which resulted in a large support rotation of  $\theta_{max} = 12^\circ$ , corresponding to “blowout”. This intense blast caused significant concrete damage and cover spalling, with the generation of significant blast fragments at failure (**Fig. 6b**).

The effect of concrete strength can next be examined in the 15M set by comparing the results of columns HSC-15M and NSC-15M. Beginning with Blast 1, the HSC column showed reduced maximum deformation (7 mm [0.3 in.]) when compared to NSC-15M (10 mm [0.4 in.]), with similar support rotations of  $0.4^\circ$  and  $0.6^\circ$ . The HSC column also had reductions of 20% and 49% in maximum and residual deformations at Blast 2 (35 psi) (see **Fig. 8b**). Both columns showed relatively low damage after this shot, with support rotations of  $\theta_{max} = 0.9^\circ$  and  $1.2^\circ$

(“superficial” and “moderate”, respectively). The use of high-strength concrete also resulted in improved control of deformations at Blasts 3-4 (100 psi), with reductions of 20% and 14% in maximum displacements (**Fig. 8c-d**). The HSC and NSC columns underwent support rotations of  $\theta_{max} = 4.5^\circ$  vs.  $4.8^\circ$  at Blast 3, with both columns experiencing concrete crushing and the formation of plastic hinges at midspan (“heavy” damage). Likewise the final shot resulted in large rotations of  $\theta_{max} = 8.1^\circ$  vs.  $9.3^\circ$ , with significant crack propagation, crushing and cover spalling, which can indeed be qualified as “hazardous” damage (**Figs. 6a & 6c**).

In summary, the results show that the response limits in modern blast codes can be used to assess the blast behavior of both high-strength concrete and normal-strength concrete columns. The results also show that the columns in both sets showed similar response characteristics, regardless of concrete type. Indeed, increasing the concrete strength ( $f_c'$ ) did not lead to more brittle failures or a reduction in ductility. In fact, moderate enhancements in displacement control (in the range of 10-20%) were observed at most test shots as the concrete strength was increased. To further demonstrate this point, **Fig. 8e** shows the blast responses of companion beams with varying concrete strengths tested by Li. et al. <sup>26</sup>. The 125 x 250 x 2400 mm (5 x 10 x 95 in.) beams were singly-reinforced with 2-No.4 bars, with  $f_c' = 58$  and 108 MPa (8.4 and 15.7 ksi) for beams C50-No.4-S and C100-No.5-S. Testing was conducted under third-point bending over a span of 2232 mm (88 in.) using a shock-tube. It can be observed that the beams show similar displacement histories, with lower displacements for the beam with 108 MPa concrete.

On the other hand, the results from Blast 4 show that HSC columns can generate significant blast fragments at failure (see high-speed stills in **Fig. 7a** and damage photos in **Fig. 6d**). Previous researchers report that the use of fibers can increase the fragmentation resistance of HSC under blast loads. For example, Luccioni et al. <sup>27</sup> found that fibers improved the spalling resistance of HSC slabs subjected to contact explosions. Similarly, Algassem et al. <sup>28</sup> reported that fibers increased the damage tolerance of HSC beams under blast loads (see **Fig. 7b** which shows the ability of fibers to control crushing and spalling). Likewise, Burrell et al. <sup>17</sup> reported that fibers were effective in reducing secondary blast fragments in normal-strength SCC columns (see **Fig. 7c** which shows the ability of fibers to reduce concrete damage in the column midspan region). Further research examining the benefits of implementing fibers in HSC columns tested under blast loads is recommended.

*Effect of seismic detailing* — As noted in the literature survey, previous research is conflicting on the effectiveness of seismic detailing to improve the blast behavior of reinforced concrete columns. The effect of this parameter in HSC columns is investigated by comparing the results of columns HSC-10M and HSC-10M-S which were built with ties spaced at  $d/2$  (75 mm [3 in.]) and  $d/4$  (38 mm [1.5 in.]), representing non-seismic and seismic designs, respectively.

The displacement response of the columns at Blast 1 to 3 can be observed in **Table 5** and **Fig. 9**. Blast 1 (17 psi) tested both columns within the elastic range and therefore both specimens showed similar responses with support rotations of  $\sim 0.5^\circ$ . The beneficial effect of seismic design can be observed at Blast 2 (35 psi) which brought the columns into the inelastic range. As shown in **Fig. 9a**, column HSC-10M-S showed significant reductions of 38% and 69% in maximum and residual deformations at this shot, with maximum support rotations of  $1.2^\circ$  vs.  $1.9^\circ$  recorded for the specimens with seismic and nominal details. Similar enhancements occurred at Blast 3 (80 psi), where the use of seismic ties reduced maximum and residual deformations by 20% and 27% (see **Fig. 9b**). Both columns showed spalling and formation of secondary fragments at failure, however damage of core concrete was relatively better controlled in the seismic specimen, with buckling of the compression bars prevented. The seismic and non-seismic columns recorded support rotations of  $\sim 6^\circ$  and  $7.6^\circ$  which qualify as “heavy” and “hazardous”.

In summary, the results show that seismic detailing can improve the blast behavior of HSC columns by reducing displacements at equivalent blasts. Similar observations have previously been reported by Burrell et al. <sup>17</sup> in normal-strength concrete columns. It should be noted that the columns in this study had relatively small cross-sections, with testing conducted under relatively low axial loads (recall that the axial load was chosen based on the nominal axial capacity of the control NSC columns). Further blast research on the effect of seismic detailing in HSC columns having large cross-sections is recommended.

*Effect of increased longitudinal steel ratio* — Increasing the longitudinal steel ratio has been reported by several researchers as an effective means to enhance the impact and blast response of flexural dominant reinforced concrete elements <sup>26</sup>. The effect of this parameter in the HSC columns was studied by comparing the results of specimens HSC-10M, HSC-#4 and HSC-15M which had reinforcement ratios of  $\rho = 1.7\%$ ,  $2.2\%$  and  $3.4\%$ , respectively. All columns in this set were built with HSC and non-seismic ties. As shown in **Fig. 10** doubling the steel ratio from 1.7% (4-10Mbars) to 3.4% (4-15M bars) resulted in improved control of displacements in the HSC columns. All columns showed similar results at Blast 1 (17 psi), however column HSC-15M reduced maximum displacement by  $\sim 50\%$  when compared to HSC-10M at Blast 2 (35 psi), with support rotations of  $0.9^\circ$  and  $1.9^\circ$  (“superficial” vs. “moderate” damage). The benefit of increased steel ratio can also be observed at Blast 3 (80 psi), with a reduction of 41% in maximum deformations when transitioning from 10M to 15M bars, with corresponding support rotations of  $7.6^\circ$  and  $4.5^\circ$  (“hazardous” vs. “heavy” damage). More importantly, this shot

caused failure of column HSC-10M. In comparison the companion with 15M bars survived this shot, with failure delayed to Blast 4 (100 psi). While noting that the columns failed at different blast intensities, more significant damage occurred in the 15M specimen when compared to the companion with 10M bars, especially in terms of the amount of spalling (**Fig. 6d**). Examining the cracking patterns, it can also be observed that more extensive diagonal cracks occurred in the column with 15M bars, which indicates an increase in shear demands. Li. et al. <sup>26</sup> previously reported that increasing the steel ratio enhanced the blast resistance of HSC beams, but also increased damage (amount of crushing and spalling). On the other hand, Algassem et al. <sup>28</sup> reported that the use of fibers was effective in reducing spalling and controlling crushing in HSC beams, regardless of steel ratio. It is also well known that fibers increase the diagonal tension capacity of concrete, which can counter increased shear demands. Further research examining the benefits of fibers in HSC columns with increased steel ratios is recommended.

*Comparing the responses of HSC and UHPC columns* — As noted in the literature survey, several recent studies have examined the blast behavior of columns designed with more advanced ultra-high performance concrete (UHPC). Since UHPC shows very high compressive strength it is of interest to compare the blast behavior of HSC and UHPC columns. **Fig. 11** compares the responses of columns HSC-10M and HSC-15M from the current study, with columns UHPC-10M and UHPC-15M from Aoude et al.<sup>20</sup> at Blasts 2-3-4. These columns had the same setup, dimensions and reinforcement details (4-10M or 4-15M bars), but were built with fiber-reinforced UHPC having  $f'_c = 138$  MPa. The fibers in the UHPC had a length of 12 mm (0.5 in.), diameter of 0.2 mm (0.008 in.) and strength of 2000 MPa (290 ksi) and were added at a volumetric ratio of 2% (160 kg/m<sup>3</sup>).

The results in **Fig. 11a-b** confirm the superior blast behavior of UHPC when compared to conventional high-strength concrete. In the 10M set, column UHPC-10M showed reductions of 48%-55% and 70%-80% in maximum and residual deformations at Blasts 2-3, with significant reductions in maximum support rotations ( $\theta_{max} = 1^\circ$  vs.  $2^\circ$  and  $3.5^\circ$  vs.  $7.6^\circ$ ), reduced damage, and an ability to sustain one more blast before failure. Indeed, the UHPC column showed no visible damage prior to failure at Blast 4, which occurred due to tension bar rupture at the critical crack (see **Fig. 11e**). The difference in failure mode can be explained by the very high toughness of UHPC in compression, coupled with its high bond capacity, which transfers failure from concrete in compression to steel in tension. Despite the brittle failure, no secondary fragments were formed at UHPC column failure.

The same trend of improved response is observed when comparing the responses of columns UHPC-15M and HSC-15M in **Fig. 11c-d**. While both columns showed similar results early on at Blast 2, the UHPC column showed reductions of 33% and 47% in maximum deformations and 70% and 67% in residual displacements at Blasts 3 and 4, with support rotations of  $\theta_{max} = 3^\circ$  vs.  $4.5^\circ$  and  $4.3^\circ$  vs.  $8.1^\circ$ . Increasing the tension steel ratio prevented bar rupture in the UHPC column at Blast 4 (**Fig. 11f**), allowing for better utilization of UHPC material capacity.

In summary, the results show that the use of UHPC results in improved blast behavior when compared to conventional HSC columns. In addition to its high-strength, UHPC contains steel fibers which provide the material with exceptional tensile resistance, toughness and damage tolerance, which translates into superior blast performance. Further research on HSC columns reinforced with steel fibers is recommended.

## ANALYTICAL INVESTIGATION

Single-degree-of-freedom (SDOF) modelling is commonly used in practice to assess the blast performance of normal-strength reinforced concrete columns <sup>4</sup>. In this study, the ability of SDOF analysis to predict the blast response of HSC columns is investigated. In this study, the dynamic resistance functions were developed using non-linear sectional analysis incorporating dynamic material properties, as described in the following sections.

### Material models

The blast response of the columns was predicted using SDOF analysis after defining the material response for concrete and steel reinforcement at high-strain rates. A summary of the models is shown in **Table 6** and **Fig. 12**.

*Concrete in compression* — The response of confined concrete in compression was modelled using the stress-strain relationship proposed by Légeron and Paultre <sup>29</sup>. This model accounts for important parameters affecting the performance of confined concrete, including the spacing, configuration and yield stress of the transverse steel, bar arrangement, and concrete strength. In this model, confinement is taken into account using a "confinement index" ( $I_E = f_{ie}/f'_{co}$ ), where the effective confining pressure ( $f_{ie}$ ) is calculated using the nominal confining pressure provided by the steel ties ( $f_t$ ), and an "effective confinement coefficient" ( $K_e$ ) which accounts for the arching action which occurs between the levels of the transverse steel in rectangular columns:

$$f_{ie} = K_e f_t \quad (1)$$

$$K_e = \frac{\left(1 - \frac{\sum w_i^2}{6c_x c_y}\right) \left(1 - \frac{s'}{2c_x}\right) \left(1 - \frac{s'}{2c_y}\right)}{1 - \rho_c} \quad (2)$$

In the above equation,  $s'$ ,  $c_x$ ,  $c_y$ ,  $\sum w_i^2$  and  $\rho_c$  represent the clear spacing between ties, the width of the concrete core in the x and y directions, the sum of the squares of the clear spacing between adjacent longitudinal bars and the ratio of longitudinal steel in the core region, respectively. The model defines the stress-strain curve using the point of peak confined strain and stress ( $\epsilon'_{cc}$ ,  $f'_{cc}$ ) and the strain at 50% drop in peak stress ( $\epsilon_{cc50}$ ,  $0.5f'_{cc}$ ), with an exponential descending branch, as described in **Table 6**.

The response of unconfined confined concrete in the cover region was simulated using the model proposed by Popovics<sup>30</sup>. The equations used in this model are summarized in **Table 6**. To account for spalling, the cover response was assumed to drop to 40%  $f'_{co}$  at a strain of 0.003, with zero stress at a strain of 0.0035.

Previous research indicates that concrete experiences an increase in strength under dynamic loading. These studies shows that compressive strength, aggregate stiffness and specimen size are factors that affect the dynamic properties of concrete (Soroushian et al.<sup>31</sup>; Bischoff and Perry<sup>32</sup>; Elfahal and Krauthammer<sup>33</sup>). Guo et al.<sup>34</sup> examined the dynamic compressive properties of three high-strength concretes with static strengths of 60, 80 and 110 MPa using a Split Hopkinson Pressure Bar (SHPB) device. Rate dependence was quantified using the dynamic increase factor (DIF), which can be defined as the ratio of dynamic to static strength. All three concretes exhibited significant rate sensitivity, with an increase in strength under dynamic loading. Samples with C60 and C80 concrete showed similar DIF, with lower values for the C110 concrete.

In the current study the CEB<sup>35</sup> equations were used to estimate the rate sensitivity of concrete since this model accounts for the influence of increased compressive strength on dynamic resistance (see **Table 6**). Using this model, and a strain-rate of  $1 \text{ s}^{-1}$  for the shock-tube tests, DIFs of 1.30 and 1.15 were determined for NSC and HSC, respectively. **Fig. 12a-b** show typical stress-strain curves for confined and unconfined concrete, with and without DIF applied. To examine the effect of DIF model, two additional analysis cases were conducted using design DIF factors for reinforced concrete columns in the far design range<sup>36</sup> (Case 2: DIF = 1.19), and ignoring dynamic effects (Case 3: DIF = 0).

*Longitudinal steel in tension and compression* — The response of the longitudinal steel reinforcement in tension was modelled using the relationships proposed by Jacques et al.<sup>37</sup>. As shown in **Table 6**, this model consisted of two linear segments to describe elastic and post-yield behavior, and a parabolic function to describe the effect of strain-hardening. Previous research indicates that reinforcing steel experiences an increase in strength under dynamic loading, with the increase in stress being greater at yield than ultimate<sup>38</sup>. To account for the effects of high-strain rates, the Saatcioglu et al.<sup>39</sup> expressions (see **Table 6**) were used to determine DIFs of 1.30 and 1.1 for steel at yield and ultimate stress (Case 1). Sample stress-strain curves with and without DIF are shown in **Fig. 12c**. Two additional analysis cases were considered, including Design DIFs of 1.17 & 1.05 at yield & ultimate<sup>36</sup> (Case 2), and ignoring dynamic effects (Case 3: DIF = 0).

Bar buckling in compression was modeled using the relationships proposed by Yalcin and Saatcioglu<sup>40</sup>, with the stability of the compression bars expressed as a function of bar aspect ratio ( $s/d_b$ ), defined as the ratio of the unsupported bar length between adjacent ties and the longitudinal bar diameter (see **Fig. 12d**).

### **SDOF analysis**

After defining the constitutive material models, the dynamic response of the columns was predicted using software *RCBlast*<sup>41</sup> by solving the equation of motion shown below:

$$K_{LM}m\ddot{u}(t) + R(u(t)) = AP_r(t) \quad (3)$$

where  $\ddot{u}(t)$  and  $u(t)$  are the acceleration and displacement at column mid-height,  $R(u(t))$  is the column resistance as a function of displacement, and  $K_{LM}$  is a load-mass factor used to transform the column into an equivalent SDOF system<sup>42</sup>. In the analysis, the mass  $m$  was taken to be 315 kg (694 lb.), equivalent to the total mass of the column and load-transfer device. The loading function was defined using the time-variant blast pressure  $P_r(t)$  and the loaded area,  $A$ , taken as area of the shock-tube end-frame opening ( $4.12 \text{ m}^2$  [ $44 \text{ ft}^2$ ]). An equivalent triangular blast load with the same peak reflected pressure and impulse recorded in the experiments was used in the analysis (see **Table 7**).

Analysis using *RCBlast* began by defining the cross-sectional properties of the columns and constitutive models for the concrete and steel reinforcement as described above. Using this data, the program computed the moment-curvature relationship of the column using sectional analysis. With the moment-curvature relationship and a user-defined plastic hinge length, the resistance functions were then computed using the lumped inelasticity approach (**Fig. 12e-f**). Detailed description of this method is provided in Jacques et al.<sup>37</sup>. The plastic hinge length at midspan and at the supports was taken to be equal to the effective depth, defined as the distance between the extreme compression fiber and tension steel bars. During testing the columns experienced a reduction in axial load during maximum response due to column shortening and associated horizontal deformations under lateral blast pressures<sup>37</sup>. To account for variable axial load, composite resistance functions were determined using 6 axial load steps

from 0 to 294 kN (66 kips) using an available function in *RCBlast*<sup>41</sup>. The load-deformation characteristics generated by the program and the previously defined idealized triangular blast loads were then used to solve the equation of motion using the average acceleration method.

### **SDOF analysis results**

**Fig. 13a** shows a sample analysis result, while **Fig. 13b** and **Table 7** compare the predicted results ( $d_{\text{anls}}$ ) and experimental maximum displacements ( $d_{\text{exp}}$ ), as well as their ratio ( $d_{\text{anls}}/d_{\text{exp}}$ ) at Blasts 1-4. Considering all columns and all blast scenarios, the average  $d_{\text{anls}}/d_{\text{exp}}$  ratio was found to be 1.04 with an average absolute error of 14%, and a coefficient of variation of 15.1%. Overall, the results show reasonable agreement between the SDOF analysis predictions and the experimental results for most of the HSC and NSC columns. Considering the individual blasts, it can be observed that the analysis under-predicted the displacements at Blast 3 (average  $d_{\text{anls}}/d_{\text{exp}}$  ratios of 1.17, 1.03 and 0.94 at Blasts 1, 2 and 3, respectively), and this can be explained by the effect of accumulated damage from repeated testing which was not considered in the analysis.

The effect of DIF model is illustrated in **Fig. 13c**, where it can be seen that ignoring strain-rate effects (DIF = 0, Case 3) and the use of constant design DIF values (Case 2) resulted in higher  $d_{\text{anls}}/d_{\text{exp}}$  ratios when compared to Case 1 (strain-rate dependent DIF models). When considering all blasts, the  $d_{\text{anls}}/d_{\text{exp}}$  ratios for Cases 1, 2 and 3 were found to be 1.04, 1.08 and 1.14, which follows the expected trend. In general, the conservative results from Case 3 confirm that dynamic material properties should be considered in the blast analysis of HSC and NSC columns. On the other hand, the use of design DIF models resulted in reasonably accurate predictions.

### **Parametric study on larger-scale columns**

After validation of the analysis methodology, the blast behavior of larger scale columns having dimensions of 3.5 m × 350 m × 350 mm (14 in. × 14 in. × 138 in.) was analyzed using the same SDOF procedure presented in the previous section. **Fig. 14a** and **Table 8** describe the design details of the columns, which had two different cross-sections (Configurations-A and B: with 8 bars + single ties and 12 bars + double-ties), three longitudinal steel ratios (use of 15M, 20M and 30M bars), three transverse steel detailing levels ( $R_d = 1.5, 2.5$  and 4.0, as defined in the CSA A23.3 standard<sup>23</sup>), with concrete strengths of 40 MPa [6 ksi] (NSC) and 80 MPa [12 ksi] (HSC). In all cases, the columns were assumed to be fully-fixed and subjected to a constant axial load corresponding to 40% of the nominal capacity of the control 40 MPa columns. Blast loads were simulated in software *RCBlast* for a constant standoff of 20 m and varying TNT charge weights, increased in 50 kg (110 lb.) increments up to 700 kg (1550 lb.) or column failure. The results of the analysis are shown in **Fig. 14**, which shows a comparison of column displacements as a function of TNT charge weight.

Beginning with the effect of concrete strength, **Fig. 14b-c** show that the use of HSC in the columns with 15M bars and  $R_d=4$  detailing reduced displacements at equivalent blasts without increasing blast resistance, which is similar to the observation in the experiments. On average, the displacements were reduced by 17% for both Configurations-A and B as the concrete strength was increased from 40 to 80 MPa.

Next, the effect of longitudinal steel ratio is examined in **Fig. 14d-e** which compares the results of the Configuration-A normal-strength and high-strength concrete columns with 15M, 20M and 30M bars ( $\rho = 1.3\%, 2\%$  and 3%). It can be seen that increasing the steel ratio reduced displacements, and increased blast resistance, for both concrete types, which is similar to the observations in the experiments.

Finally, the effect of transverse steel detailing in the HSC columns can be examined in **Fig. 14f-g**. No significant differences in performance are observed when varying detailing in the HSC columns at the early blasts, however the use of “ductile” ( $R_d = 4.0$ ) detailing increased blast capacity and delayed column failure in both Configurations-A and B. Moreover, it can be observed that improving the detailing within the cross-section (i.e. use of double ties vs. single ties [Type B vs. A]) allowed for greater blast capacity, especially for the columns with  $R_d = 2.5$  detailing. As noted before, the scaled columns in the experimental study had relatively small cross-sections; based on the observations in the numerical study, further blast research examining the effect of transverse steel detailing in HSC columns have large cross-sections is recommended.

## **SUMMARY, FINDINGS AND CONCLUSIONS**

This paper presented the experimental results from six columns built with normal-strength concrete and high-strength concrete which were tested under simulated blast loading using a shock-tube. The tests examined the effects of concrete strength, seismic detailing and longitudinal reinforcement ratio on blast response. The following conclusions can be drawn from this study:

1. The results showed that the use of high-strength concrete did not significantly affect the blast response of the columns, in terms of blast capacity or failure mode when compared to normal-strength concrete.